Science of the Total Environment 691 (2019) 572–583

Contents lists available at ScienceDirect

Science of the Total Environment

journal homepage: www.elsevier.com/locate/scitotenv

Plutonium and other radionuclides persist across marine-to-terrestrial ecotopes in the Montebello Islands sixty years after nuclear tests

M.P. Johansen [a,*], D.P. Child [a], T. Cresswell [a], J.J. Harrison [a], M.A.C. Hotchkis [a], N.R. Howell [a], A. Johansen [a], S. Sdraulig [b], S. Thiruvoth [a], E. Young [a], S.D. Whiting [c]

[a] ANSTO, Sydney, Australia
[b] Australian Radiation Protection and Nuclear Safety Agency, Yallambie, Australia
[c] Department of Biodiversity, Conservation and Attractions, Kensington, WA, Australia

HIGHLIGHTS

- 1950s nuclear tests have left a legacy of long-lived radionuclides.
- Today, the sites have high value as marine and terrestrial habitats.
- Pu is persistent, but in variable amounts across marine-to-terrestrial ecotopes.
- The dominant Pu in all marine and terrestrial wildlife was locally-sourced.
- Pu remains a long-term exposure concern to human visitors and wildlife.

GRAPHICAL ABSTRACT

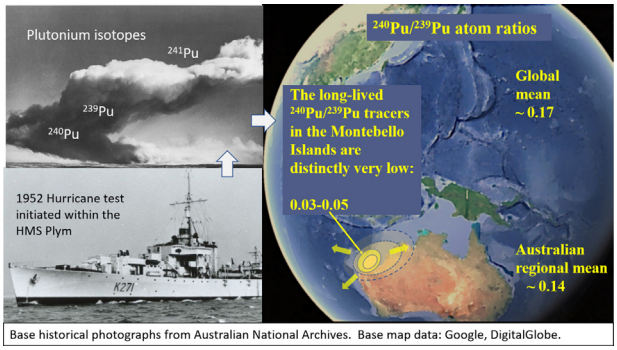

Base historical photographs from Australian National Archives. Base map data: Google, DigitalGlobe.

ARTICLE INFO

Article history:
Received 12 April 2019
Received in revised form 29 June 2019
Accepted 30 June 2019
Available online 2 July 2019

Editor: Mae Sexauer Gustin

Keywords:
Pu atom ratio
Caesium-137
Marine
Biota
Radioactive particles
Radioecology

ABSTRACT

Since the 1956 completion of nuclear testing at the Montebello Islands, Western Australia, this remote uninhabited island group has been relatively undisturbed (no major remediations) and currently functions as high-value marine and terrestrial habitat within the Montebello/Barrow Islands Marine Conservation Reserves. The former weapons testing sites, therefore, provide a unique opportunity for assessing the fate and behaviour of Anthropocene radionuclides subjected to natural processes across a range of shallow-marine to island-terrestrial ecological units (ecotopes). We collected soil, sediment and biota samples and analysed their radionuclide content using gamma and alpha spectrometry, photostimulated luminescence autoradiography and accelerator mass spectrometry.

We found the activity levels of the fission and neutron-activation products have decreased by ~hundred-fold near the ground zero locations. However, Pu concentrations remain elevated, some of which are high relative to most other Australian and international sites (up to 25,050 Bq kg^{-1} of $^{239+240+241}$Pu). Across ecotopes, Pu ranked from highest to lowest in the following order: island soils > dunes > foredunes > marine sediments > and beach intertidal zone. Low values of Pu and other radionuclides were detected in all local wildlife tested including endangered species. Activity concentrations ranked (highest to lowest) terrestrial arthropods > terrestrial mammal and reptile bones > algae > oyster flesh > whole crab > sea turtle bone > stingray and teleost fish livers > sea cucumber flesh > sea turtle skin > teleost fish muscle. The three detonations (one from within a ship and two from 30 m towers) resulted in differing contaminant forms, with the ship detonation producing the highest activity

* Corresponding author.
E-mail address: Mathew.Johansen@ansto.gov.au (M.P. Johansen).

https://doi.org/10.1016/j.scitotenv.2019.06.531

concentrations and finer more inhalable particulate forms. The three sites are distinct in their $^{240/239}$Pu and $^{241/239}$Pu atom ratios, including the Pu transported by natural process or within migratory living organisms.

1. Introduction

In October 1952, a nuclear weapon with a plutonium core was detonated in the hull of the HMS Plym, which was anchored in shallow waters within the Montebello Islands off of Western Australia. The 25 kt detonation initially caused a gamma burst, quickly followed by pressure and heat waves, which drew vaporised and molten materials from the ship, seawater, seafloor sediments up into a rising thermal cloud. The subsequent radioactive fallout was deposited first onto local waters and islands, then, with less intensity, regionally and ultimately across northern Australia (Butement et al., 1957; Child and Hotchkis, 2013; Lal et al., 2017; Tims et al., 2013; Tims et al., 2016).

This test, code-named Hurricane, initiated the British nuclear testing program and was the first major atmospheric release of anthropogenic radionuclides in the Southern Hemisphere. Two additional nearby nuclear detonations followed four years later, Mosaic G1 and Mosaic G2, the latter being the largest of all nuclear detonations of the British tests in Australia (the proposed yield was 60 kt, estimates of the actual yield approach 100 kt: Child and Hotchkis, 2013; UNSCEAR, 2000).

The legacy of radionuclides generated by these three 1950s tests creates a unique opportunity for study. In the 60+ years since the detonations, the island test sites have been relatively undisturbed. The remote Montebello Islands have low usage from humans with minimal industrial activities. No substantial construction or remediation activities have been undertaken, leaving the radionuclide residuals to be acted upon only by the natural forces from marine currents and tides, weather events and erosion. The relatively undisturbed condition of the islands, as well as their oceanographic and climatic profiles, provide for exceptional habitat for a diverse range of biota including endangered fauna. The island group supports resident and nesting green hawksbill and flatback sea turtles, and resident loggerhead turtles. Additionally, each major island serves a refuge for critically-endangered mammals (Langford and Burbidge, 2001; Pendoley et al., 2016; Whiting et al., 2009; Whiting et al., 2008).

Despite the high ecological value of the islands, major gaps exist in the knowledge of the nature, extent, and environmental behaviour of the residual radionuclides in island soils and waters. Other similar sites, such as Bikini Atoll, have been comparatively disturbed by decommissioning and clean-up operations and other human activities (Bordner et al., 2016). At the Montebello Islands, some data exist from decades-old government surveys that were last conducted in the 1980s (Australian Radiation Laboratory (ARL) Report Series; ARL, 1979; ARL, 1980; ARL, 1982; ARL, 1983; ARL, 1990). The final 1990 report of the series highlighted ongoing plutonium (Pu) contamination. However, these past government surveys provided no data on the marine system except for a few potential human food items. No data are available on marine sediments or uptake into marine fish, for example. While the Montebello Island nuclear tests are frequently mentioned in review publications on nuclear testing (Prăvălie, 2014; Simon and Bouville, 2002), we found less than one dozen novel radionuclide data from the Montebello Islands in peer-reviewed science publications (mainly from Child and Hotchkis, 2013).

This study aims to fill these gaps using a novel approach that compares the persistence of plutonium and other radionuclides across marine-to-terrestrial ecological units. Its primary objectives were to:

- Determine activity concentrations of radionuclides in environmental materials (e.g. soils, sands and sediments) across a range of ecotopes in relatively undisturbed conditions.
- Document persistence and mobility (e.g. via erosion processes) of residual radionuclides over time.
- Estimate uptake of key radionuclides in wildlife species, with an emphasis on marine organisms.
- Determine the ratios of Pu isotopes and the Pu:Am activity concentration ratios among the three test sites.

The resulting data are intended to inform evaluations on the persistence and spreading of long-lived radionuclides, the uptake of these radionuclides in endangered species that use the islands (e.g. flatback turtle), and regional, southern-hemisphere and global evaluations where Pu, in particular, is used as a relatively new, but long-lived tracer that can be measured at extremely low levels.

2. Materials and methods

2.1. Site description

The Montebello Islands are a group of more than two hundred distinct islands and islets that lie 85 km off the coast of Western Australia. The climate is arid and hot, with annual rainfall averaging 320 mm (Government of Western Australia, 2007). The marine region is characterised by strong currents, and the islands can be subjected to extreme weather events such as cyclones, with wind gusts exceeding 250 km/h, although fringing reefs somewhat protect littoral zones within the islands. Sublittoral habitats are typically sand/soft-bottom, and shorelines are often shallow limestone platforms interspersed with sandy beaches. Foredune and dune areas on larger islands have intermittent, patchy vegetation coverage that, inland, is dominated by *triodia* and scrubby *acacia* (Government of Western Australia, 2007).

Due in part to their remote location, the British Government selected the islands as a testing location for its emerging nuclear weapons program in May 1951. The first test (Hurricane Test; ~25 kt) was performed in October 1952 using a device that was detonated 2.7 m below the waterline within the HMS Plym vessel anchored in approximately 12 m seawater between Trimouille and Alpha Islands (Fig. 1). The detonation deposited highly radioactive fallout in the immediate lagoon area and the central-western portion of Trimouille Island, with lesser amounts deposited on other islands and still lower amounts along the northern WA coastal region and across northern Australia (Child and Hotchkis, 2013; Tims et al., 2013). In 1956, two additional Pu-weapons were detonated from 30 m towers, Mosaic G1 (~15 kt) and Mosaic G2 (~60–100 kt). After the tests, many structures were removed, and ~1.5 m plinths were emplaced at ground zero locations, but there was no substantive cleanup of residual contamination (ARL, 1982; ARL, 1983).

2.2. Sampling

This study's sampling design sought to, for the first time, characterise radionuclides across island marine, intertidal beach and dune areas as well as update the decades-old data for the terrestrial island soils. Our study design included samples gathered from within the fallout deposition areas of the three test sites (Fig. 1) and across the distinct ecological functional units (ecotopes): sublittoral marine zones (seawater and marine sediments), intertidal beach areas, foredunes (supralittoral), dunes, and island soils.

Samples of marine sediments, beach sands and soils were from the top 10 cm or less to document the radionuclides most available to

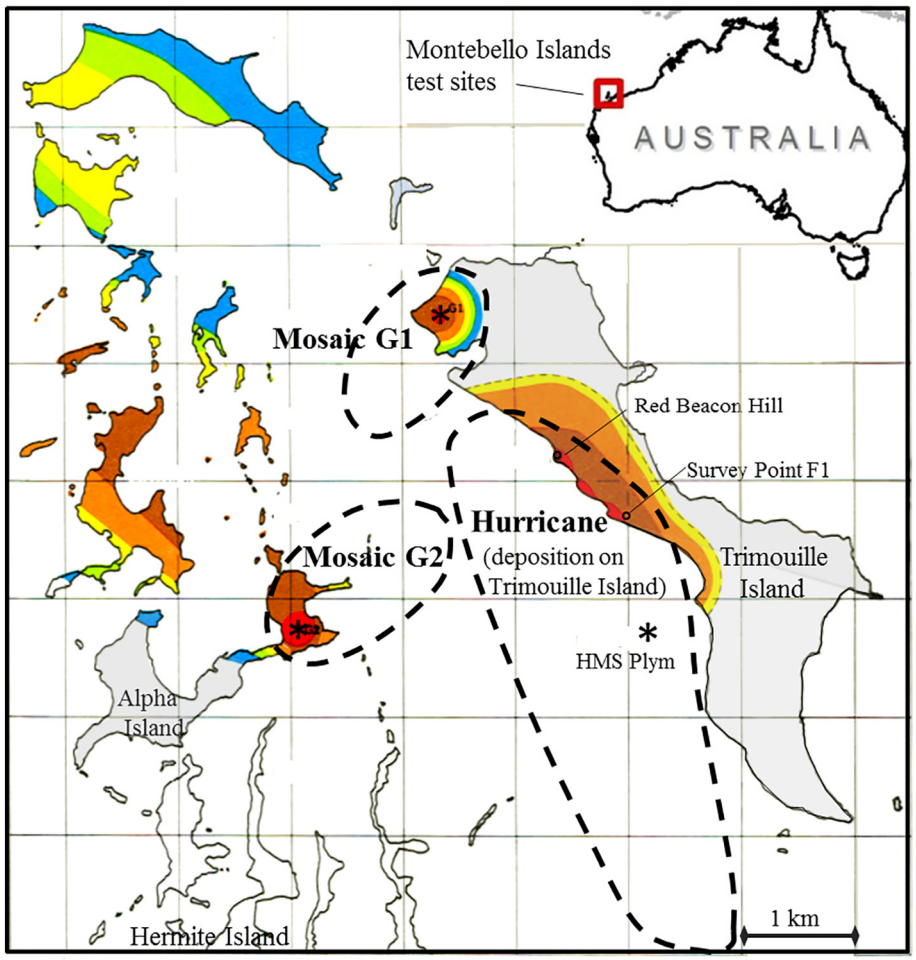

Fig. 1. Primary 2015 sampling areas (dashed lines) superimposed on the 1962 survey gamma map (blue-yellow–red increasing gamma emissions; ARL, 1982). Detonation locations are indicated by * symbols. Additional 2015 sampling was conducted on other locations including at Claret Bay at the southern end of Hermite Island approximately 10 km south of the Mosaic G2 site.

human and wildlife receptors. Marine sediment samples were collected using a Van Veen grab sampler. Sediments were collected into sealed plastic bags and kept cool (<4 °C) until analysis. Soils and beach sands were gathered using a 50 mm PVC tube, or similar method, to ensure uniform depth representation.

Radiocaesium in seawater was extracted, in-situ, by pumping 1000 L seawater through two cartridges (in series) that were chemically coated with potassium copper hexacyanoferrate. The water was collected at a depth of 1 m and pre-filtered through a 1-μm filter cartridge. The two coated cartridges were then ashed and the ash counted in standard geometry containers for 96–110 h by high-resolution gamma spectrometry as described in Bokor et al. (2016).

Tissue samples were collected from a range of biota including algae, sea cucumber (*Holothuria spp.*), oyster (*Saccostrea spp.*), sea turtle (*Natator depressus*), blue spotted ray (*Taeniura lymma*), a range of teleost fish and arthropods (see Section 3.4). Due to their protected status, island reptiles and mammals could not be sampled conventionally and the few samples that were obtained did not provide replication within species. Bones were collected opportunistically from a limited number of deceased monitor lizards (*Varanus gouldii*) and island mammals (*Bettongia lesueur*, *Lagorchestes hirsutus*). Collection was by conventional means (e.g. hand and net collection, fishing line) under wildlife license and animal ethics approvals. All tissue samples were washed (vigorously rinsed in a series of three DI water baths) to minimise the retention of externally-adhered contamination. Sea cucumbers were depurated live for >12 h in clean seawater to void undigested food items. Gut contents were collected and analysed separately.

A gamma dose-rate survey was undertaken using a RadEye™ B20 Multi-Purpose Survey Meter with gamma probe (Thermo Scientific) along transects previously surveyed at G1 and G2 sites by ARL between 1962 and 1990 (ARL, 1980; ARL, 1982; ARL, 1990). Gamma dose-rates were recorded at 1 m above the ground every 25 m distance from the detonation site (Mosaic G2; Fig. S1) following cardinal transects (i.e. N, NE, E, etc.).

Comparative samples were gathered from Claret Bay, located in the southernmost area of the island group. This comparison site was the furthest (~10 km) site from the test areas that was available, but still within the Montebello Islands group. The Claret Bay site was not expected to be completely free of Montebello test influence (not expected to represent background conditions) as historical information suggested the tests deposited some contamination regionally across western and northern Australia (Butement et al., 1957; Tims et al., 2016). However, no previous radiological data for distal areas of the Montebello Islands were available. For regional comparison, additional samples were gathered on mainland coastal areas (e.g. near Karratha, near Geraldton, WA). Samples were gathered in November 2015 (all data are decay corrected to this date) and >190 laboratory analyses were performed in addition to in-situ field measurements (Table S1).

2.3. Laboratory analysis methods

2.3.1. Alpha spectrometry

Surface soils and marine sediments were screened to remove fragments, coarse pebbles and vegetation (>500 μm). The bulk soil was

then homogenised, and a subsample was taken (~10 g). Dried or ashed samples were digested prior to analysis using a three-step digestion process: aqua regia reflux (solid:liquid ratio 1:20, 108 °C, 4 h); open hotplate digestion using hydrofluoric acid; and fusion digestion of residual solids (IAEA, 2010b). Any residue remaining after digestion was collected on a filter paper and screened for total radioactivity (ISO, 2009). Radioactivity was not detected above instrument background in these residues indicating adequate dissolution of the sample matrices.

Sample digests were spiked with yield tracers ^{232}U (EZA Source 83609-657), ^{229}Th (EZA Cat. No. 7229), ^{242}Pu (NIST SRM 4334I), ^{243}Am (EZA Cat. No. 7243) and stable Sr. Autochthonous stable Sr concentrations in each sample were measured by ICP-AES and taken into consideration in the Sr yield assessment. Samples were chemically processed as described in Harrison et al. (2011). Uranium (^{238}U, ^{234}U), Thorium (^{230}Th; to assess for potential U components to the 1950s testing), plutonium ($^{239+240}$Pu, ^{238}Pu) and americium (^{241}Am) were measured by alpha spectrometry on a Canberra Alpha Analyst using Passivated Implanted Planar Silicon (PIPS®) detectors as described in Harrison et al. (2016).

For measurement of ^{210}Po in biota, the samples were dried and ground as above, then were spiked with a known amount of ^{209}Po tracer and digested using concentrated HNO_3 followed by a mixture of concentrated HNO_3 and hydrogen peroxide. The polonium was separated from the matrix using a manganese dioxide precipitation. The precipitate was dissolved, and the polonium was auto-deposited onto silver discs prior to measurement using alpha spectrometry (ARPANSA, 2015).

2.3.2. Beta analysis

Digests for beta analysis were conducted as described for alpha spectrometry. Strontium-90 (^{90}Sr) was quantified by Cherenkov counting (L'Annunziata and Kessler, 2012) on a Perkin-Elmer Tri-Carb 3100TR liquid scintillation counter. Instrumentation settings and count methodology are described in Harrison et al. (2011).

2.3.3. Gamma spectroscopy

Gamma-emitting radionuclides in soils and sediments were measured using an ORTEC High-Purity Germanium (HPGe) n-type reduced background detector (relative efficiency of 45%) coupled to an ORTEC DSPEC Pro with MAESTRO software. An equivalent geometry, soil matrix, mixed gamma calibration source (15 × 55 mm, EZA SRS 94204) was used for energy and efficiency calibration across an energy range of 46.5–1836.1 keV. Dried and homogenous samples were counted between 24 and 72 h each to achieve adequate counting statistics.

The gamma-emitting radionuclides in biota samples were measured in standard-geometry containers using Canberra High Purity Germanium n-type detectors with associated Canberra Genie 2000 software. The detectors were calibrated using multi gamma calibration standard. The samples were dried and ground prior to measurement.

Spatial mapping of gamma emissions at the Mosaic G2 site was accomplished using a portable gamma-ray spectroscopy system with a customised analysis algorithm. Data were acquired by carrying the system in an approximate grid pattern over the geographical area of interest while acquiring 10s gamma spectra. Data are reported on the net peak counts of ^{152}Eu and ^{137}Cs in each spectrum using a region of interest specific to each radionuclide and a linear background approximation for background subtraction (see Flynn et al. (2016) for details).

2.3.4. Accelerator mass spectrometry (AMS)

Surface soils and sediments were screened to remove soil particles over 500 μm, coarse pebbles and vegetation. The bulk soil was then homogenised, and a subsample was taken (~1 g). The soil/sediment was weighed into a porcelain crucible and dried at 60 °C overnight. The dried sample was then heated to 800 °C in a muffle furnace for 3 h to ensure the destruction of organic material. The combustion residue was again weighed to determine the loss on ignition and transferred to a 50 mL Savillex PFA Block Digestion tube with 100 fg (100E-15 g) of NIST 4224H ^{242}Pu as an isotope dilution tracer. Soils and sediments were then leached in 10 mL of aqua regia at 108 °C for 3 h. This leachate was fumed dry with HNO_3 to remove chlorine and then decanted. The residue was rinsed with HNO_3 (with the rinse added to the leachate) and then fully digested with 10 mL of a 1:1 mixture of HNO_3 and HF. HF was removed from the digest solution by multiple fumings with HNO_3 at 108 °C, and 0.5 mL of 0.66 M Boric acid added to complex residual fluoride. All sample leaching, digestion and fuming steps were completed in sealed vessels under a 0.1 μm filtered, high purity airflow to prevent cross-contamination. The leachate and digest fractions were combined, and the redox conditions adjusted to produce Pu^{4+} ions. These combined fractions were then applied to Eichrom industries 2 mL TEVA resin cartridges and purified by extraction chromatography. A purified plutonium fraction was eluted after removal of matrix contaminants.

Biota samples were weighed into porcelain crucibles and dried at 60 °C overnight. The dried samples were then heated to 800 °C in a muffle furnace for 3 h to ensure the complete destruction of organic material. The combustion residue was again weighed to determine the loss on ignition, and transferred to a 50 mL Savillex PFA Block Digestion tube with 100 fg (100E-15 g) of NIST 4224H ^{242}Pu added as an isotope dilution tracer. The ashed residue was digested in 10 mL of aqua regia at 108 °C for 3 h. The digest was fumed dry with HNO_3 to remove HCl and then decanted. Leaching and fuming steps were completed in sealed vessels under a 0.1 μm filtered, high purity airflow to prevent cross-contamination. The digest solutions were diluted with 3 M HNO_3 to ensure dissolution of inorganic salts, and the redox conditions adjusted to produce Pu^{4+} ions. These combined fractions were then applied to Eichrom industries 2 mL TEVA resin cartridges and purified by extraction chromatography. A purified plutonium fraction was eluted after removal of matrix contaminants.

All acids used were Seastar IQ grade that had been further cleaned using Savillex sub-boiling distillation rigs. All other reagents used were ultra-high purity (e.g. Sigma Aldrich Trace-select) unless otherwise stated.

2.5 mg of iron as iron nitrate (high purity standards 10M26-2 10000 ppm single element standard, purified by extraction through Eichrom 2 mL UTEVA resin cartridge) was added and a co-precipitate formed with plutonium by NH_3 neutralisation. Fe—Pu co-precipitates were centrifuged, dried at 60 °C and calcined at 600 °C to form a pellet of iron oxide. These were mixed 1:1 with −325 mesh niobium powder and loaded into a cathode for measurement. AMS sample targets were loaded into a metallic sample holder (cathode) with a capacity of <10 mg of solid, conductive sample material.

The samples were measured on the VEGA 1MV AMS facility (Wilcken et al., 2015) at ANSTO, following the method described in detail in Hotchkis et al. (2018). Actinide isotopes were injected into the AMS system as monoxide negative ions with injection energy of 60 kV with the terminal voltage set to 0.68 MV. Helium was used as stripping gas in the terminal and resulted in charge state yields of around 40% for 3+ ions while operating with sufficient gas pressure to ensure complete destruction of molecules. After acceleration, all plutonium isotopes were measured as count rates in an ion chamber following three medium-resolution analysis steps: first magnetic, second electrostatic and third magnetic, ensuring excellent background suppression. Isotopes of interest were injected and analysed sequentially using fast electrostatic switching in a one-second cycle (^{239}Pu: 100 ms; ^{240}Pu: 400 ms; ^{241}Pu: 400 ms; ^{242}Pu: 100 ms). Isotope ratios were measured relative to the spike (^{242}Pu) and normalised to ratios measured with standard reference materials. Instrument and process blanks were used to apply background corrections.

2.3.5. Photostimulated luminescence (PSL) autoradiography

Soil and sediment samples were mixed (1:3 ratio) with a 10%*w*/*v* sugar solution and affixed in a thin uniform layer to a clean

20cmx40cm Perspex plate by oven drying. A uniform high-density polyethylene film was placed over the surface of the sample, followed by an imaging phosphor plate (BAS-SR 2040, Fujifilm™). Sample and plate were exposed in a darkened chamber for six days. Plates were read on a FLA7000 (General Electric) variable mode laser scanner and tiff files processed using FIJI (Image J).

3. Results and discussion

3.1. Persistence of Pu

At most locations tested, the 2015 activity concentrations of radionuclides measured in soils and sediments rank (highest to lowest) $^{239+240+241}$Pu > ^{137}Cs > ^{90}Sr > ^{241}Am > ^{152}Eu > $^{234+238}$U > ^{230}Th > ^{60}Co, although some variation exists due to heterogeneous spatial distribution. The single highest $^{239+240+241}$Pu value, 25,050 Bq kg^{-1} (mean of nearby samples = 17,700 Bq kg^{-1}; Fig. 2) is the highest recently-reported Pu value from Australian surface soils (Johansen et al., 2014) and is comparable to the highest measurements from archived samples from Mosaic G2 (Child and Hotchkis, 2013) collected as part of the 1972 and 1978 ARL sampling campaign. It is >100,000 times higher than background levels elsewhere in Australia (range of 0.02–0.50 Bq kg^{-1}; Child and Hotchkis, 2013; Hancock et al., 2011; Smith et al., 2016). The highest 2015 Pu data are orders of magnitude higher than that reported for areas contaminated by the Fukushima accident (<1 Bq kg^{-1}; Zheng et al., 2013) and the first nuclear test at the Trinity site (typically up to 5 Bq kg^{-1}, but up to 2500 Bq kg^{-1} at ground zero in the 1970s and 80s; Hanson and Rodgers, 1985; Nyhan et al., 1976). They are somewhat higher than Pu levels at comparable (<10 km) distances from the post-accident Chernobyl NPP (Eric, 1997) and those at the Palomares accident site (Jimenez-Ramos et al., 2006); and comparable to many, but less than some data from the Semipalatinsk site (Nápoles et al., 2004).

This sample with the highest Pu in soil was found within the Hurricane test deposition zone on Trimouille Island, approximately 1.5 km from the ship detonation site (mean of nearby samples = 17,700 Bq kg^{-1}; Fig. 2). Despite the Mosaic G2 detonation being an estimated 4 times larger in terms of the explosive yield than Hurricane ship detonation (~100 kt compared to 25 kt), its residual Pu values in the soil samples from near ground zero are an order of magnitude lower (Fig. 2). This likely reflects a combination of factors including the lower altitude particle distribution of the Hurricane test due to the water-based platform and the water vapour condensation scavenging of fallout giving rise to higher local fallout. Each of the three test sites, however, has pervasive and persistent Pu at levels that are orders of magnitude above background (Fig. S2). All, including the comparatively minor Mosaic G1 site, have Pu levels above the 100 Bq kg^{-1} International Atomic Energy Agency (IAEA) guidance level for the general release of material to the public (IAEA, 2005).

On inland island soils, the data indicate the persistence of Pu with little attenuation due to natural processes. The Pu activity concentrations are similar when comparing 2015 to 1972 data gathered from the same

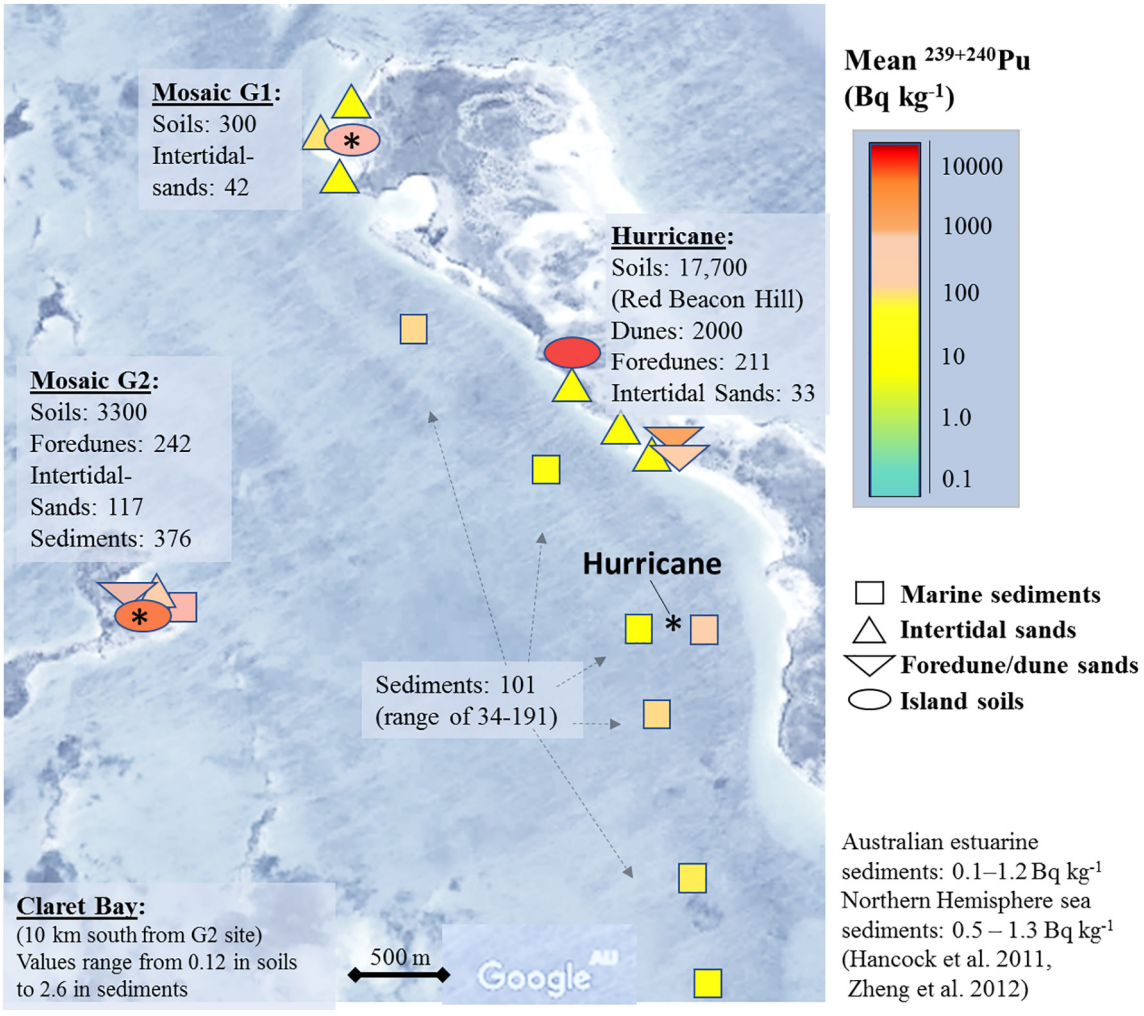

Fig. 2. Mean $^{239+240}$Pu activity concentrations (Bq kg^{-1}) from soils, sand, and sediment samples. Means are from multiple data in Tables S3, S4, S5; some sediment and sand activity concentrations were calculated from ^{241}**Am using the activity concentration ratios measured in this study. Detonation locations are indicated by . symbols.**

approximate locations (Red Beacon Hill and Survey Point F1, Fig. 1 and Table S2). However, establishing trends over time is hampered by the uncertainty of the 1972 locations, which are detailed on maps, but not by GPS. Also, comparisons between studies are difficult, because the soil radionuclides are distributed heterogeneously, in part due to variation in their initial deposition patterns, and also due to the presence of particles. Because of this heterogeneity, it is probable that further systematic sampling will reveal higher Pu levels in Montebello soils.

Samples from marine sediments also indicate persistent Pu and other radionuclides, although at lower activity concentrations than island soils (Fig. 2). The $^{239+240}$Pu in seabed sediment samples collected between Trimouille and Alpha Islands is elevated on average nearly four orders of magnitude above background (Fig. 2). The mean of the Pu in marine sediments near the G2 site is 376 Bq kg^{-1} (Fig. 2), which is higher than or comparable to activity concentrations in various marine nuclear sites in the Arctic (Skipperud, 2004), and is higher than the value of 99 Bq kg^{-1} recently reported for sediments in the Bikini Lagoon of the Pacific Proving Ground (Buesseler et al., 2018). The sediment Pu levels along a transect crossing the Hurricane detonation site (HMS Plym, Fig. 2) ranged from 34 to 191 Bq kg^{-1} (mean of 101 Bq kg^{-1}) that are comparable with the Bikini site data. It is significant that the Pu levels in marine sediments at the Montebello and Bikini sites are similar given that only three tests were conducted at Montebello while 23 tests were conducted at the Bikini site, (many of which were orders of magnitude larger). However, the sediment Pu levels measured in this study are about one order of magnitude lower than the maximums in sediments at the Thule accident site (Dahlgaard et al., 2001; Ikäheimonen et al., 2002). Pu is elevated in all sediment samples from the 5+ km transect across the HMS Plym site including the southernmost sample from near the edge of the island group (Fig. 2). This suggests the sites act as ongoing sources for contaminated sediment plumes that may extend for many kilometres outside the island area. The extent of this dispersion remains an important question related to Pu isotopic signatures in regional sediments and wildlife as well as the use of Pu as a tracer in marine systems.

3.2. Decrease of short-lived radionuclides

The persistence of the long-lived Pu contrasts with the short-lived radionuclides, particularly those at ground zero locations where the measured gamma emissions have decreased sharply over time. For example, gamma emissions in the vicinity of Mosaic G1 and G2 ground zero sites (Fig. S1) have decreased by factors approaching 100 in the past +60 years. At these locations, much of the gamma dose rate in the past came from the neutron-activation products found predominantly in soils and rocks within ~hundred metres from ground zero. The neutron activation products ^{60}Co and ^{152}Eu have half-lives of 5.3 and 13.5 years respectively and have largely decayed away (with less than one atom in 5000 and one atom in 40 remaining, respectively). Because of these highly localised neutron activation products, the rapid reduction rates observed at ground zero are heightened (faster) as compared with other island locations where neutron activation did not directly occur.

The main point revealed by comparing activity concentrations and dose rates over time is that the easily measured gamma emissions have decreased sharply in a matter of decades, particularly those near ground zero locations. However, the Pu and other long-lived actinides persist in marine sediments and island soils with slow reduction and ongoing spreading over time.

3.3. Radiological gradients across ecotopes

We found that the key residual radiological contaminants (e.g. Pu) vary in concentration by three orders of magnitude across marine-to-terrestrial ecotopes. Activity concentrations are typically lowest at the seawater-beach interface and increase progressively inland (highest to lowest: inland soils > dune sands > foredune sands > intertidal sands). Marine sediments have higher activity concentrations than the intertidal beach sands for most radionuclides (Fig. 3).

The higher Pu persistence at inland soil sites is consistent with evidence of relatively slow erosion and transport rates at the Mosaic G2 detonation site, Alpha Island. Gamma contaminant patterns from 1962 (ARL, 1982) are roughly similar to those from 2015, with both exhibiting higher activity concentrations to the NE and SW of ground zero (Fig. 4). However, the data of Fig. 4 suggest that in the past fifty-three years there has been a limited eastward shift of 10s of metres in the approximate centroid of the ^{137}Cs contamination according to radionuclide-specific gamma mapping (Fig. 4; Flynn et al., 2016). Such a shift would be consistent with erosion and transport downslope along the localised west-to-east topographic gradient. A similar shift is not as apparent for the ^{152}Eu (Fig. 4) that is consistent with the understanding the ^{152}Eu, as a neutron-activation product, was primarily created in-situ, and is therefore mostly embedded in the subsurface soils/rocks. Thus, the ^{152}Eu is expected to have more limited movement than the ^{137}Cs fission product that was deposited on the ground surface from fallout and is more susceptible to surface erosion. It is probable that the Pu isotopes are being transported at rates similar to ^{137}Cs as they both have high particle adsorption affinities and both were deposited as fallout. The data suggest there will be ongoing erosional transport and input to the local marine system of Pu isotopes and ^{137}Cs as well as other soil-adsorbed radionuclides.

The ecotope-radionuclide profiles indicate greater cumulative erosion and transport occurrence in supra-littoral/intertidal areas that receive routine scour from waves and tides. We estimate 45–55% of Pu that originally deposited above the low tide line on Trimouille Island has been transported into the sea over the past sixty-three years as determined by comparing a 1952 Pu deposition pattern based on the historical gamma deposition maps from ARL (1982) with the 2015 soils data; although more detailed study, including additional spatial soil sampling, is needed to refine this estimate. The mobilisation rates of sediment-attached radionuclides during cyclones would be high at these sites, particularly on Trimouille Island where the radioactivity is mostly in very-fine particulate form with only a few discernible particles of >0.01 mm evident (Fig. 5; Pu and Cs have relatively high particle affinity, see Bellenger and Staunton, 2008; IAEA, 2004; IAEA, 2010a). The detonation aboard the HMS Plym occurred 2.7 m below the water line and ~9 m above the seafloor (Cathcart, 1994) and therefore would have incorporated mainly water vapour and sea salts, with some contribution from ship and sediment materials, leading to the formation of fine salt aerosol particles in the radioactive fallout.

In comparison, the soil samples from near Mosaic G2 had more abundant and relatively large radioactivity bearing particles (up to ~1 mm) which appear typical of other near-surface fission tests in which most of the elements taken up into the radioactive cloud came from the soils immediately below the test tower (Salbu, 2001; Salbu et al., 2017). This tower detonation occurred 30 m above the terrestrial surface, composed predominantly of a calcareous and ferruginous limestone soil some of which would have been excavated during the detonation and incorporated, along with weapon and tower structure residues, into the fallout matrix. However, no large fused-glassy fragments (so-called “blast glass”) were observed.

The difference in particle sizes within Hurricane and Mosaic G2 test fallout also offers an explanation for levels of Pu found in the sediments near the detonation sites (Fig. 5). Due to their tower release mode that entrained soils (e.g. Ca and Si compounds), the G2 particles are larger and more resistant to erosion and persist longer in the marine environment compared to the particles generated by the Hurricane test that are finer (more easily transported) and Fe-dominated (more easily oxidised and corroded). The finer particles on Trimouille Island are also higher in activity (Fig. 5). They can pose higher dose potential to humans and wildlife because they are more easily entrained into the atmosphere if

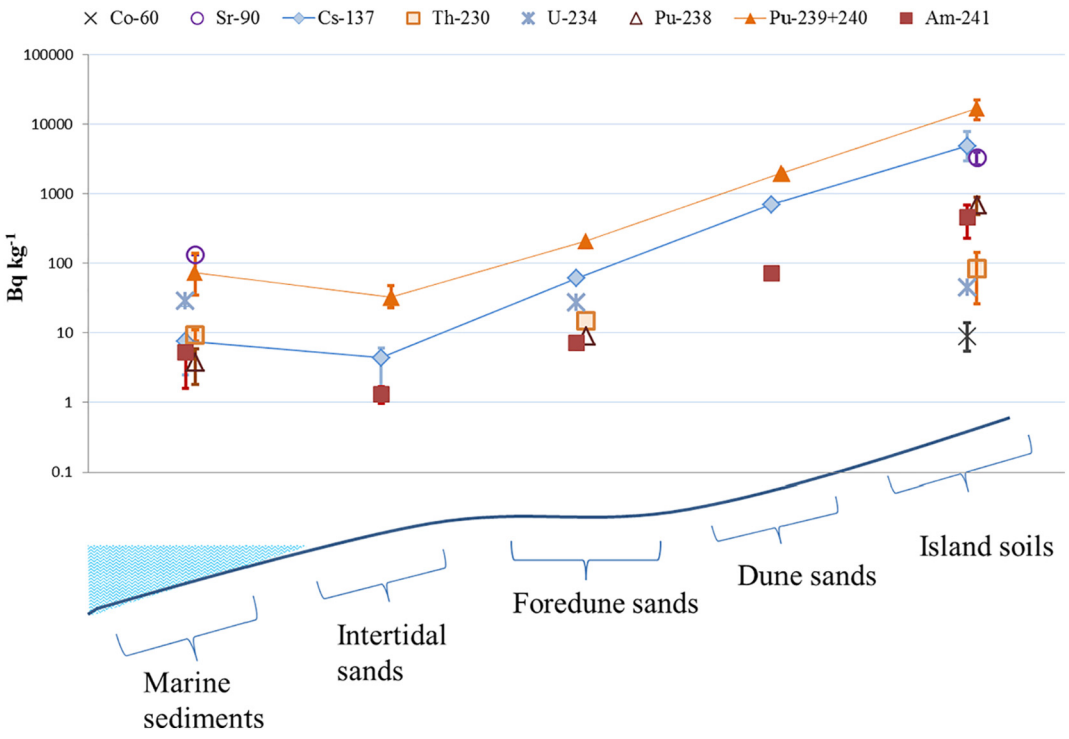

Fig. 3. Activity concentrations in surface soils, sands, and sediments (<10 cm) across study ecotopes in the Hurricane deposition area of Trimouille Island. Lines shown for $^{239+240}$Pu and ^{137}Cs data. For this area, ^{152}Eu was below detection limits (see Tables S3, S4, and S5 for data).

the soil is disturbed, and more easily inhaled, leading to higher rates of transfer to the lungs of humans and animals.

The gradients across ecotopes also reflect the relative solubility of the radionuclides. Cs ions, in particular, have enhanced solubility when moved from terrestrial to marine conditions due to competition for binding sites by other 1^+ cations, mainly K^+ in seawater (IAEA, 2004). However, some ^{137}Cs can remain particle-attached in marine conditions for many years (Kusakabe et al., 2017), and slowly solubilise and mobilise in seawater (the ^{137}Cs activity concentrations in seawater near the detonation sites were similar to that from the control site at Claret Bay; Table S3). In contrast, ^{90}Sr that was in rough parity with ^{137}Cs in island soil, did not experience the same increased solubility when moved to marine conditions (Takata et al., 2014). While the activity concentrations of all the radionuclides are less in the marine sediments than in the island soils, ^{137}Cs decreases the most and ^{90}Sr decreases the least. In the marine sediments near Trimouille Island, the highest measured activity concentration was for ^{90}Sr (higher than Pu). This has implications for dose to wildlife as living organisms readily take up ^{90}Sr (Rosenthal et al., 1972; Tsukada et al., 2005), and the energetic beta emission from its progeny ^{90}Y contributes to dose (Delacroix et al., 2002).

3.4. Uptake of radionuclides into wildlife tissues

Pu isotopes and other radionuclides persist above background levels in all local organisms tested. Pu activity concentrations ranked (highest to lowest) island arthropods > island mammals and reptiles > algae > oyster flesh > whole crab > turtle bone > stingray and teleost fish livers > sea cucumber flesh > turtle skin > teleost fish muscle (Supplemental Tables S4 and S5). The relative concentrations in biota reflect the ecotope profiles discussed above (Section 3.3) indicating the soils and sediments act as ongoing sources for other ecosystem elements.

Fish liver data indicate that Pu levels are, on average, higher in those species that have diets associated with sediment/benthos organisms. The highest fish liver $^{239+240}$Pu result (of $n = 7$) was from a spangled emperor (*Lethrinus nebulosus*), sampled from waters between the test

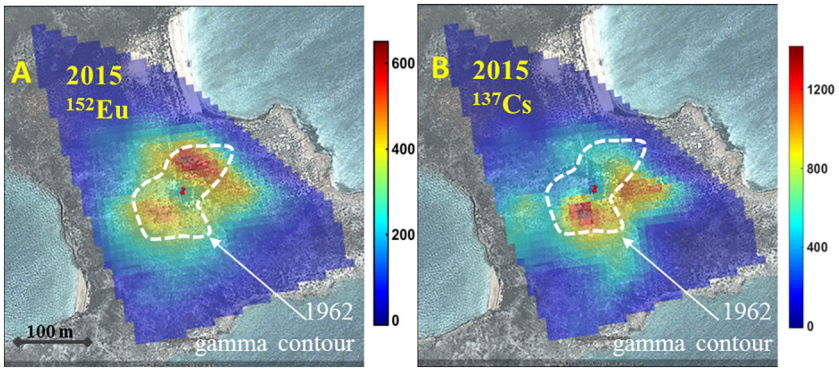

Fig. 4. Spatial mapping of gamma emissions at the Mosaic G2 site based on ^{152}Eu (A) and ^{137}Cs (B) from the 2015 field survey (counts per ten-second acquisitions, see methods section). For comparison, a contour of the 1962 dose rate survey (50 μSv hr^{-1}; ARL, 1982) is superimposed which suggests an south-eastward shift of ^{137}Cs in surface soils has occurred over the past fifty-three years.

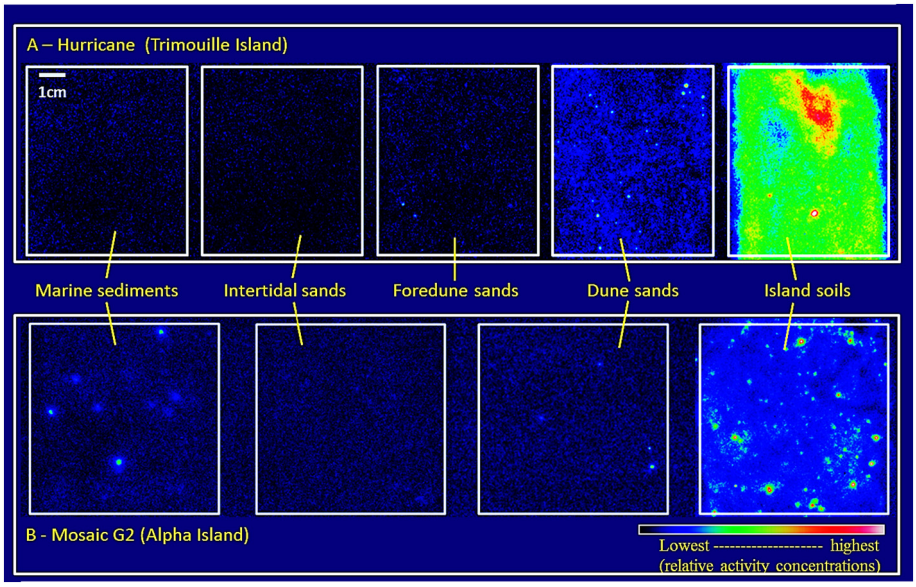

Fig. 5. PSL Autoradiography of sediment-sand-soil subsamples of 3 g for each panel. Top (A) is from the Hurricane deposition site near Red Beacon Hill on Trimouille Island. The bottom (B) is from the Mosaic G2 site, Alpha Island.

areas (0.57 ± 0.01 Bq kg^{-1} fresh mass). Spangled emperors feed on molluscs, crustaceans, polychaete worms and other sediment-associated prey (Froese and Pauly, 2000). Goatfish (*Upeneichthys spp.*) and blue spotted ray (*T. lymma*) also feed on benthic organisms and also had relatively elevated $^{239+240}$Pu compared with that in the livers of upper-trophic level carnivores captured in the same area, such as coral trout (*Plectropomus leopardus*). These data are consistent with other studies indicating that Pu does not biomagnify in marine food chains (Noshkin et al., 1997; Skwarzec et al., 2001).

The Pu activity concentrations in fish muscle samples were approximately one order of magnitude lower than that in the liver from the same fish. The $^{239+240}$Pu results in the edible flesh of non-migratory bentho-pelagic feeders from near the test sites (e.g. spangled emperor 0.002–0.003 Bq kg^{-1} muscle fresh mass) are higher than the reference ambient Pu levels in muscle of similar marine fish reported from the Northern Hemisphere (mean = 0.0002, SD = 0.0001, n = 7 N. Atlantic, $n = 3$ N. Pacific; Nagaya and Nakamura, 1987; Noshkin, 1972; Noshkin et al., 1979). However, from a risk/dose perspective, consumers of muscle tissues from these fish would receive an increase in dose from the Pu many orders of magnitude lower than that from the natural radionuclides in the same fish such as ^{210}Po (e.g. committed effective doses of 7.5E-7 mSv from $^{239+240}$Pu compared with 1.5E-3 mSv from ^{210}Po from ingestion of 1 kg of fish muscle using the values in Table 1). When considering ^{137}Cs levels in fish muscle (Table 1), we found no evidence of increased dose/risk from ^{137}Cs levels in game fish caught in the Montebello islands compared to ambient background levels. Although the $^{239+240}$Pu and ^{137}Cs in fish muscle are detectable using highly sensitive instruments, the fish at the Montebello Islands contain much greater concentrations of natural than anthropogenic radionuclides as is typical of marine fish around the world (Aarkrog, 2003; Johansen et al., 2015).

Compared with fish, Pu was higher in the filter feeders (oyster) and organisms that are in routine contact with sediments (algae, and sea cucumber). Oysters feed by filtering suspended particles as well as dissolved constituents (Lee et al., 2015). Oyster flesh samples from near the test sites had elevated Pu by 1–2 orders of magnitude over the levels from the comparison site at Claret Bay (Supplemental Fig. S3). Low levels of ^{137}Cs, ^{152}Eu and ^{241}Am were also present in oyster flesh from near the test sites (Table S3 and S4).

Pu in algae samples from between Trimouille and Alpha Islands was elevated by more than an order of magnitude as compared with the sample from Claret Bay, and two orders of magnitude higher than algae sampled 190 km to the east near the mainland at Dampier, WA (Supplemental Fig. S3).

Sea cucumbers feed by ingesting and drawing nutrients from sediments passing through their stomach and intestinal tracts. Pu in depurated tissues (dominated by epidermis, dermis and muscle tissues) was three orders of magnitude lower than the gut contents, which

Table 1
Activity concentrations ^{137}Cs, ^{210}Po, $^{239+240}$Pu and Pu atom ratios in fish tissues (fresh mass). All values decay corrected to 1 November 2015. The uncertainties (±) include systematic and statistical errors and correspond to one standard deviation.

	^{137}Cs in muscle Bq kg^{-1}	^{210}Po in muscle Bq kg^{-1}	$^{239+240}$Pu in muscle Bq kg^{-1}	$^{239+240}$Pu in liver Bq kg^{-1}	^{240}Pu/^{239}Pu atom ratio (liver data)
Coral trout (Claret Bay)	0.24 ± 0.02	0.25 ± 0.01	0.003 ± 0.001	0.0172 ± 0.0002	0.045 ± 0.002
Coral trout (between Alpha and Trim. Islands, $n = 2$)	0.24 ± 0.02	0.26 ± 0.01	nm	0.0174 ± 0.0002	0.043 ± 0.003
Spangled emperor (between Alpha and Trim. Islands, n = 2)	0.13 ± 0.02	1.28 ± 0.07	0.004 ± 0.002	0.5694 ± 0.0050	0.037 ± 0.001
Goatfish (between Alpha and Trim. Islands, comp = 4)	0.19 ± 0.02	5.9 ± 0.3	nm	0.1005 ± 0.0009	0.040 ± 0.002
Stingray (between Alpha and Trim. Islands, n = 3)	0.15 ± 0.01	10.0 ± 0.3	nm	0.0791 ± 0.0008	0.038 ± 0.001

nm = not measured.

suggests very low uptake absorption fractions (*f* value of approximately 0.0014), and may be due in part to the low soluble particle forms discussed above (Section 3.3).

Plutonium concentrations measured within terrestrial organisms were significantly higher than those found in marine organisms (Tables S4 and S5). Results included 6.7 Bq kg^{-1} $^{239+240}$Pu in a primitive spider (*Mygalomorphae spp.*) and 97.0 Bq kg^{-1} in a wolf spider (*Lycosidae spp.*) collected from within 100 m of Mosaic G2 ground zero location (Fig. 1). A cockroach (*Blattidae spp.*) from the same location had even higher concentrations, at 380 Bq kg^{-1}. The higher levels in the wolf spider and cockroach are likely due to their frequent contact with the ground surface, while the primitive spider was collected from a web that separated it from the ground surface. Ants collected near the Mosaic G1 site had the highest Pu levels of all arthropods at 1270 Bq kg^{-1} $^{239+240}$Pu. While all specimens were vigorously washed and rinsed, it is probable that a portion of the Pu measured was from contamination adhered to or embedded in their exoskeleton rather than internal tissues.

Of the mammals and reptiles, the burrowing bettong (*Bettongia lesueur*) bones from near (<100 m) the Mosaic G2 ground zero (Fig. 1) had the highest $^{239+240}$Pu levels (10 Bq kg^{-1}), while the rufus hare-wallaby (*Lagorchestes hirsutus*) and sand goanna (*Varanus gouldii*) bones from near Mosaic G1 had lower concentrations (0.6 and 1.1 Bq kg^{-1} $^{239+240}$Pu). These limited samples suggest higher uptake by mammals in the Montebello Islands compared with those from the Pu-contaminated test sites at Maralinga on the Australian mainland (0.02–2.1; whole-body Bq kg^{-1} in *Macropus rufus* and *Oryctolagus cuniculus* (Johansen et al., 2016)). The relative Pu levels in bones at Mosaic G1 and G2 roughly mirror that of their respective soils, with Mosaic G2 being about one order of magnitude higher. Due to their protected/endangered status, no mammal or reptile bones were recovered during fieldwork in the Hurricane deposition areas on Trimouille Island, which would be expected to have the highest activity concentrations based on respective soil activity concentrations. The limited data suggest additional study using non-lethal sampling is warranted on these species as they have substantive Pu body burdens and their small remaining populations are limited mainly to these contaminated island refuges.

3.5. Isotopic atom ratios and activity concentration ratios

The isotopic ratios of ^{240}Pu/^{239}Pu and ^{241}Pu/^{239}Pu indicate distinct signatures among the Montebello test sites, and all three had markedly different Pu isotopic composition from worldwide fallout (Table 2; Krey et al., 1976a, 1976b). The Hurricane and Mosaic G1 ratios have not been previously published, and the atom ratio data for Mosaic G2 from this study agree well with the previously published value based on archived samples (^{240}Pu/^{239}Pu atom ratio of 0.05 (±0.004); Child and Hotchkis, 2013). The ratios in Table 2 were measured from 2015 soil samples gathered near (50 m) the ground zero locations of Mosaic G1 and G2 and, for the Hurricane test, at Red Beacon Hill of Trimouille Island (Fig. 1) which historical surveys suggest had a relatively high deposition from the ship-based test.

Since the different Pu isotopes are nearly chemically indistinguishable (e.g. have similar adsorption/desorption), the original ratios persist through time and can be used, for example, to help identify the source of archived historical items gathered from the Montebello Islands or nearby areas. The Pu atom ratios in biological samples can be used to distinguish samples locally among the three test sites (Fig. 6). For example, sea turtle eggshells absorb nutrients and contaminants from their host beach sands during incubation. Eggshell samples from near G2 on Alpha Island have a mean ^{240}Pu/^{239}Pu atom ratio of 0.049 (±0.003); while those associated with the Hurricane test site at Main Beach have a lower atom ratio of 0.027 (±0.001). Fish samples gathered from shallow seawater areas between the detonation sites, by contrast, indicate mixtures of Pu from the various sites. The distinct signatures of samples from the different test sites can be further established using the ^{241}Pu/^{239}Pu atom ratios (Table 2) as well as the ^{238}Pu/$^{239+240}$Pu activity ratios (from data in Table S4), both of which indicate the variation between the sites and can be useful as distinct tracers. However, the ^{241}Pu/^{239}Pu atom ratios have relatively large counting errors due to the extremely small amounts of ^{241}Pu remaining in the 2015 samples, which reflects the proportionally small amounts of ^{241}Pu initially generated as well as its relatively short 14.3-year half-life. The $^{239+240}$Pu/^{241}Am activity concentration ratios from the Montebello sites (Table 2) appear to be distinctly higher than those from other testing from the same time period at Maralinga (Johansen et al., 2014).

All biota samples gathered within the Montebello Islands group indicated some influence of Pu sourced locally from the Montebello tests. Pu from the tests was manifest in all samples from Claret Bay area 10 km SW at the southern edge of the island group including in relatively fixed soils samples as well as mobile fish samples. While the levels of Pu in these samples from the Claret Bay areas are low (approximately similar to background reference levels), their Pu has ^{240}Pu/^{239}Pu and ^{241}Pu/^{239}Pu atom ratios that fall distinctly within the envelope of the three local tests (Fig. 6, Table 2) as compared with that of global fallout (from reference values in Kelley et al. (1999) and Krey et al. (1976b) corrected to the date of sampling 11/2015). This finding is not surprising as the tests were known to deposit fallout not just locally, but also regionally (Butement et al., 1957). Our data confirm this, as, for example, a surface soil sample from Eaglehawk Island, 95 km to the east of the test sites, had a ^{240}Pu/^{239}Pu atom ratio of 0.027 (±0.001) indicating substantial fallout contribution from the Montebello tests. Soil samples from near Geraldton, WA (from 940 km south) had ^{240}Pu/^{239}Pu atom ratios of 0.10 (±0.01), which also indicates some contribution from

Table 2
Isotopic and activity concentration ratios of Pu and Am from 2015 soil samples (means; see Supplemental Tables S4 and S5 for data). All values decay corrected to 1 November 2015. The uncertainties (±) include systematic and statistical errors and correspond to one standard deviation.

	^{240}Pu/^{239}Pu activity concentration ratio	^{239}Pu/^{241}Am activity concentration ratio	$^{239+240}$Pu/^{241}Am activity concentration ratio	^{240}Pu/^{239}Pu atom ratio	^{241}Pu/^{239}Pu atom ratio
Mosaic G1 (N. Trimouille Isl.)	0.135 ± 0.005	16.8 ± 0.7	19.1 ± 0.8[a]	0.037 ± 0.002	1.9E-05 ± 4.7E-05
Mosaic G2 (Alpha Isl.)	0.193 ± 0.007	12.4 ± 0.6	14.8 ± 0.7[a]	0.053 ± 0.003	3.2E-05 ± 8.0E-05
Hurricane (Trimouille Isl.)	0.100 ± 0.003	26.9 ± 1.4	29.5 ± 1.5[a]	0.027 ± 0.001	1.0E-05 ± 4.6E-05
Eaglehawk Isl., WA	0.10 ± 0.03	0.22 ± 0.02	0.24 ± 0.03	0.027 ± 0.001	4.4E-05 ± 8.0E-05
Geraldton, WA	0.37 ± 0.02	0.10 ± 0.01	0.14 ± 0.03	0.102 ± 0.009	7.2E-05 ± 3.5E-04
Global average				0.176[b]	8.7E-04 −9.0E-04[c]

[a] Using 2015 $^{239+240}$Pu values from AMS and ^{241}Am from alpha spectrometry. When the Pu and Am values from alpha spectrometry were used, the $^{239+240}$Pu:^{241}Am ratios were slightly lower at G1 = 18.2, G2 = 13.4, Hurricane = 28.5.
[b] (Krey et al., 1976b).
[c] Range (Kelley et al., 1999).

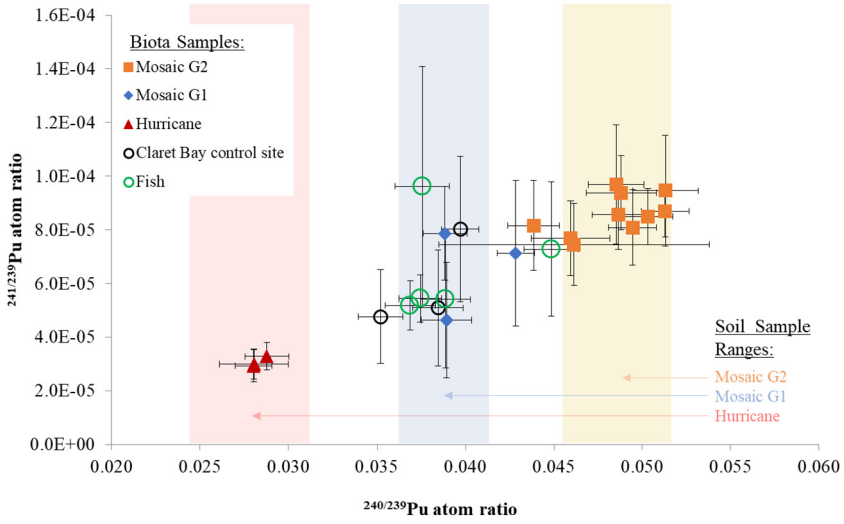

Fig. 6. $^{241/239}$Pu vs $^{240/239}$Pu atom ratios from biota samples identified by their respective collection sites, except for the fish samples which were gathered from seawater areas between detonation sites. Only data from samples with sufficient mass to result in uncertainties <50% are graphed (see Table S5 for data). For comparison, the ranges of $^{240/239}$Pu ratios are shaded as measured in soil samples from the Hurricane (red), Mosaic G1 (blue), Mosaic G2 (orange) sites.

Montebello islands weapons testing, although contribution from other British tests in South Australia is also possible at this latitude (Child and Hotchkis, 2013; Tims et al., 2016). Hirose and Aoyama (2003) have documented that the Southern Ocean ^{240}Pu/^{239}Pu ratios in seawater are low relative to those of the Northern Hemisphere. Their finding is consistent with the results of this study which establish the Montebello ^{240}Pu/^{239}Pu atom ratios as being very low (0.027–0.053) relative to global means (Table 2) and document substantial input of this Montebello Pu into the Southern Hemisphere marine system, especially from the Hurricane ship test from which sediment Pu levels remain elevated 60+ years later. Our data is the first to document this substantive transfer of Montebello Pu in the Southern Hemisphere marine system, the contribution of which to ocean tracers studies may yet be fully realised (Lindahl et al., 2010).

3.6. Future research

While this work produced >600 analytical results across a range of ecological media types (Supplement), there are many remaining knowledge gaps due to the ecological complexity of the islands and the physicochemical variation in the range of radionuclides involved. Future research should focus on marine sediments (extent of radionuclide sediment plumes and their interactions with corals and benthic organisms), the occurrence and nature of radioactive particles, the use of Pu isotopic ratios as biological markers for local and migrating species, the investigation of current and past dose rates to organisms such as sea turtles that undergo early development while incubating in radionuclide-contaminated sands and those endangered mammal species whose diminished populations are confined mainly to the contaminated islands.

4. Conclusions

The activity concentrations of fission and neutron activation products near the ground zero locations of Montebello Island tests have decreased ~100-fold in the past 60 years. However, Pu remains elevated with little attenuation in site soils with activity concentrations typically ranking (highest to lowest) $^{239+240+241}$Pu > ^{137}Cs > ^{90}Sr > ^{241}Am > ^{152}Eu > $^{234+238}$U > ^{230}Th > ^{60}Co. Across ecotopes, the Pu and other radionuclides rank (highest to lowest) island soils > dunes > foredunes > marine sediments > and beach intertidal zone (three orders of magnitude lower than site soils). Data indicated erosion and island-to-sea transport of radionuclides over time. Numerous discrete particles were found, mostly in site soils, but also in beach and sediment samples. The particles from the Hurricane ship-based test are finer and of higher activity concentrations than those from the two Mosaic tower tests. These differences appear to be influencing the transport and longevity of particles in the local environment.

All marine and terrestrial organisms had Pu signatures dominated by local Pu (vs stratospheric fallout Pu). Pu and other radionuclides were detected in all local wildlife tested, with activity concentrations ranked (highest to lowest) island arthropods > island mammals and reptiles > algae > oyster flesh > whole crab > turtle bone > stingray and teleost fish livers > sea cucumber flesh > turtle skin > teleost fish muscle.

The three detonations resulted in differing $^{240/239}$Pu atom ratios that were distinguishable by AMS in abiotic and biotic samples from the three sites. The median $^{240/239}$Pu atom ratios in all samples from Montebello Islands (0.04) are distinct from that of Australian regional (~0.14) and global fallout (0.17–0.18). As Pu is long-lived (24,000-year half-life for ^{239}Pu), our results provide an ecosystem-based data baseline that will be useful for reference far into the future.

Acknowledgements and Funding Sources

The study was made possible by funding for sample analysis provided by the Western Australian Department of Biodiversity, Conservation and Attractions as well as laboratory support from the Australian Radiation Protection and Nuclear Safety Agency. We acknowledge financial support from the Australian Government for the Centre for Accelerator Science at ANSTO through the National Collaborative Research Infrastructure Strategy (NCRIS). Substantial work on this project was provided by Emma Davis, Lida Mokhber-Shahin, Kerry Wilsher, Alison Flynn, David Boardman and Ilonka Bokor. Rachael Marshall and other staff of the Western Australia Government enabled the study. We thank Chad and the other helpful staff of Blue Lightning Charters.

CRediT authorship contribution statement

M.P. Johansen: Conceptualization, Investigation, Data curation, Project administration, Writing - original draft. **D.P. Child:** Formal analysis, Investigation, Methodology, Conceptualization. **T. Cresswell:** Investigation. **J.J. Harrison:** Formal analysis, Data curation. **M.A.C. Hotchkis:** Formal analysis, Data curation. **N.R. Howell:** Formal analysis, Data curation. **A. Johansen:** Formal analysis, Writing - review & editing, Validation. **S.**

Sdraulig: Formal analysis, Data curation, Investigation. **S. Thiruvoth:** Formal analysis, Methodology. **E. Young:** Investigation, Methodology. **S.D. Whiting:** Investigation, Resources.

Appendix A. Supplementary Material

Supplementary data to this article can be found online at https://doi.org/10.1016/j.scitotenv.2019.06.531.

References

Aarkrog, A., 2003. Input of anthropogenic radionuclides into the World Ocean. Deep Sea Res., Part II 50, 2597–2606.

ARL, 1979. Residual Radioactive Contamination of the Monte Bello Islands From Nuclear Weapons Tests Conducted in 1952 and 1956. Australian Radiation Laboratory, Melbourne, Australia.

ARL, 1980. Field and Analytical Data Relating to the 1972 and 1978 Surveys of Residual Contamination of the Monte Bello Islands and Emu Weapons Test Sites. Australian Radiation Laboratory, Melbourne, Australia.

ARL, 1982. In: Laboratory AR (Ed.), Environmental Radiation at the Monte Bello Islands From Nculear Weapons Tests Conducted in 1952 and 1956. Australian Government, Melbourne, Australia.

ARL, 1983. The Radiological Status of the Monte Bello Islands: May 1983. Australian Radiation Laboratory, Melbourne, Australia.

ARL, 1990. Radiological Hazard Assessment at the Monte Bello Islands. Australian Government, Melbourne, Australia.

ARPANSA, 2015. Background Radioactivity in Northern Australian Seafood. Technical Report Series No. 172. 619 Lower Plenty Road Yallambie VIC 3085, Australia.

Bellenger, J.P., Staunton, S., 2008. Adsorption and desorption of ^{85}Sr and ^{137}Cs on reference minerals, with and without inorganic and organic surface coatings. J. Environ. Radioact. 99, 831–840.

Bokor, I., Sdraulig, S., Jenkinson, P., Madamperuma, J., Martin, P., 2016. Development and validation of an automated unit for the extraction of radiocaesium from seawater. J. Environ. Radioact. 151, 530–536.

Bordner, A.S., Crosswell, D.A., Katz, A.O., Shah, J.T., Zhang, C.R., Nikolic-Hughes, I., et al., 2016. Measurement of background gamma radiation in the northern Marshall Islands. Proc. Natl. Acad. Sci. 113, 6833–6838.

Buesseler, K.O., Charette, M.A., Pike, S.M., Henderson, P.B., Kipp, L.E., 2018. Lingering radioactivity at the Bikini and Enewetak Atolls. Sci. Total Environ. 621, 1185–1198.

Butement, W.A.S., Dwyer, L.J., Eddy, C.E., Martin, L.H., Titterton, E.W., 1957. Radioactive fallout in Australia from operation mosaic. 20 (5).

Cathcart, B., 1994. Test of Greatness - Britain's Struggle for the Atom Bomb. John Murray, London.

Child, D.P., Hotchkis, M.A.C., 2013. Plutonium and uranium contamination in soils from former nuclear weapon test sites in Australia. Nucl. Inst. Methods Phys. Res. B 294, 642–646.

Dahlgaard, H., Eriksson, M., Ilus, E., Ryan, T., McMahon, C.A., Nielsen, S.P., 2001. Plutonium in the marine environment at Thule, NW-Greenland after a nuclear weapons accident. In: Kudo, A. (Ed.), Radioactivity in the Environment. vol. 1. Elsevier, pp. 15–30.

Delacroix, D., Guerre, P.J., Leblanc, P., Hickman, C., 2002. Radionuclide and radiation protection data handbook 2002. Radiat. Prot. Dosim. 98, 1–168.

Eric, V., 1997. The radiological consequences of the Chernobyl accident. Environ. Rev. 5, 203–205.

Flynn, A., Boardman, D., Sarbutt, A., Reinhard, M., Young, E., 2016. Mapping Montebello Islands using a portable gamma-ray spectroscopy system. 2016 IEEE Symposium on Radiation Measurements and Applications. University of Michigan, US.

Froese, R., Pauly, D., 2000. In: Froese, R., Pauly, D. (Eds.), FishBase 2000: Concepts, Design and Data Sources. ICLARM, Los Baños, Laguna, Philippines, p. 344.

Government of Western Australia, 2007. In: Conservation DoEa (Ed.), Management Plan for the Montebello/Barrow Islands Marine Conservation Reserves 2007–2017. Western Australia. Dept. of Environment and Conservation Kensington, W.A.

Hancock, G.J., Leslie, C., Everett, S.E., Tims, S.G., Brunskill, G.J., Haese, R., 2011. Plutonium as a chronomarker in Australian and New Zealand sediments: a comparison with ^{137}Cs. J. Environ. Radioact. 102, 919–929.

Hanson, W.C., Rodgers, J.C., 1985. Radiological Survey and Evaluation of the Fallout Area from the Trinity Test: Chupadera Mesa and White Sands Missile Range, New Mexico. Los Alamos National Laboratory, Los Alamos, NM, USA.

Harrison, J.J., Zawadzki, A., Chisari, R., Wong, H.K.Y., 2011. Separation and measurement of thorium, plutonium, americium, uranium and strontium in environmental matrices. J. Environ. Radioact. 102, 896–900.

Harrison, J.J., Payne, T.E., Wilsher, K.L., Thiruvoth, S., Child, D.P., Johansen, M.P., et al., 2016. Measurement of (233)U/(234)U ratios in contaminated groundwater using alpha spectrometry. J. Environ. Radioact. 151 (Pt 3), 537–541.

Hirose, K., Aoyama, M., 2003. Present background levels of surface ^{137}Cs and (239,240)Pu concentrations in the Pacific. J. Environ. Radioact. 69, 53–60.

Hotchkis, M.A.C., Child, D.P., Froehlich, M., Wallner, A., Wilcken, K., Williams, M., 2018. Actinides AMS on the VEGA accelerator. Nucl. Inst. Methods Phys. Res. B 438, 70–76.

IAEA, 2004. Sediment Distribution Coefficients and Concentration Factors for Biota in the Marine Environment (TRS 422). International Atomic Energy Agency, Vienna, AUT.

IAEA, 2005. In: IAEA (Ed.), Derivation of Activity Concentration Levels for Exclusion, Exemption and Clearance. International Atomic Energy Agency, Vianna, Austrial.

IAEA, 2010a. Handbook of Parameter Values for the Prediction of Radionuclide Transfer in Terrestrial and Freshwater Environments (TRS 472). International Atomic Energy Agency, Vienna, Austria.

IAEA, 2010b. A Procedure for the Rapid Determination of Pu Isotopes and Am-241 in Soil and Sediment Samples by Alpha Spectrometry. International Atomic Energy Agency, Vienna.

Ikäheimonen, T.K., Ilus, E., Klemola, S., Dahlgaard, H., Ryan, T., Eriksson, M., 2002. Plutonium and americium in the sediments off the Thule air base, Greenland. J. Radioanal. Nucl. Chem. 252, 339–344.

ISO, 2009. ISO 18589-6:2009 Measurement of Radioactivity in the Environment - Soil - Part 6: Measurement of Gross Alpha and Gross Beta Activities. International Organization for Standardization. International Organization for Standardization.

Jimenez-Ramos, M.C., Garcia-Tenorio, R., Vioque, I., Manjon, G., Garcia-Leon, M., 2006. Presence of plutonium contamination in soils from Palomares (Spain). Environ. Pollut. 142, 487–492.

Johansen, M.P., Child, D.P., Davis, E., Doering, C., Harrison, J.J., Hotchkis, M.A., et al., 2014. Plutonium in wildlife and soils at the Maralinga legacy site: persistence over decadal time scales. J. Environ. Radioact. 131, 72–80.

Johansen, M.P., Ruedig, E., Tagami, K., Uchida, S., Higley, K., Beresford, N.A., 2015. Radiological dose rates to marine fish from the Fukushima Daiichi accident: the first three years across the North Pacific. Environ. Sci. Technol. 49, 1277–1285.

Johansen, M.P., Child, D.P., Caffrey, E.A., Davis, E., Harrison, J., Hotchkis, M.A.C., et al., 2016. Accumulation of plutonium in mammalian wildlife tissues following dispersal by accidental-release tests. J. Environ. Radioact. 151, 387–394.

Kelley, J.M., Bond, L.A., Beasley, T.M., 1999. Global distribution of Pu isotopes and ^{237}Np. Sci. Total Environ. 237-238, 483–500.

Krey, P.W., Hardy, E.P., Pachucki, C., Rourke, F., Coluzza, J., Benson, W.K., 1976a. Mass Isotopic Composition of Global Fall-out Plutonium in Soil. International Atomic Energy Agency (IAEA): IAEA.

Krey, P.W., et al., 1976b. Mass Isotopic Composition of Global Fall-out Plutonium in Soil. Transuranium Nuclides in the Environment. IAEA, Vienna, Austria, pp. 671–678.

Kusakabe, M., Inatomi, N., Takata, H., Ikenoue, T., 2017. Decline in radiocesium in seafloor sediments off Fukushima and nearby prefectures. J. Oceanogr. 73, 529–545.

Lal, R., Fifield, L.K., Tims, S.G., Wasson, R.J., 2017. (239)Pu fallout across continental Australia: implications on (239)Pu use as a soil tracer. J. Environ. Radioact. 178-179, 394–403.

Langford, D., Burbidge, A., 2001. Translocation of Mala (Lagorchestes Hirsutus) from the Tanami Desert, northern territory to Trimouille Island, Western Australia. Australian Mammal. 23, 37–46.

L'Annunziata, M.F., Kessler, M.J., 2012. Chapter 7 - liquid scintillation analysis: principles and practice. In: L'Annunziata, M.F. (Ed.), Handbook of Radioactivity Analysis, Third edition Academic Press, Amsterdam, pp. 423–573.

Lee, J.H., Birch, G.F., Cresswell, T., Johansen, M.P., Adams, M.S., Simpson, S.L., 2015. Dietary ingestion of fine sediments and microalgae represent the dominant route of exposure and metal accumulation for Sydney rock oyster (Saccostrea glomerata): a biokinetic model for zinc. Aquat. Toxicol. 167, 46–54.

Lindahl, P., Lee, S.-H., Worsfold, P., Keith-Roach, M., 2010. Plutonium isotopes as tracers for ocean processes: a review. Mar. Environ. Res. 69, 73–84.

Nagaya, Y., Nakamura, K., 1987. ^{239,240}Pu and ^{137}Cs concentrations in some marine biota, mostly from the seas around Japan. Nippon Suisan Gakkaishi 53, 873–879.

Nápoles, H.J., León Vintró, L., Mitchell, P.I., Omarova, A., Burkitbayev, M., Priest, N.D., et al., 2004. Source-term characterisation and solid speciation of plutonium at the Semipalatinsk NTS, Kazakhstan. Appl. Radiat. Isot. 61, 325–331.

Noshkin, V.E., 1972. Ecological aspects of plutonium dissemination in aquatic environments. Health Phys. 22, 537–549.

Noshkin, V.E., Wong, K.M., Eagle, R.J., 1979. Plutonium concentrations in fish and seawater from Kwajalein Atoll. Health Phys. 37, 549–556.

Noshkin, V.E., Robison, W.L., Wong, K.M., Brunk, J.L., Eagle, R.J., Jones, H.E., 1997. Past and present levels of some radionuclides in fish from Bikini and Enewetak atolls. Health Phys. 73, 49–65.

Nyhan, J.W., Miera, F.R., Neher, R.E., 1976. Distribution of plutonium in trinity soils after 28 years 1. J. Environ. Qual. 5, 431–437.

Pendoley, K.L., Whittock, P.A., Vitenbergs, A., Bell, C., 2016. Twenty years of turtle tracks: marine turtle nesting activity at remote locations in the Pilbara, Western Australia. Aust. J. Zool. 64, 217–226, 10.

Prăvălie, R., 2014. Nuclear weapons tests and environmental consequences: a global perspective. Ambio 43, 729–744.

Rosenthal, H.L., Cochran, O.A., Eves, M.M., 1972. Strontium content of mammalian bone, diet and excreta. Environ. Res. 5, 182–191.

Salbu, B., 2001. Actinides associated with particles. In: Kudo, A. (Ed.), Plutonium in the Environment; Proceedings of the Second International Symposium. vol. 1. Elsevier, pp. 121–138.

Salbu, B., Kashparov, V., Lind, O.C., Garcia-Tenorio, R., Johansen, M.P., Child, D.P., et al., 2017. Challenges associated with the behaviour of radioactive particles in the environment. J. Environ. Radioact. 186, 101–115.

Simon, S., Bouville, A., 2002. Radiation Doses to Local Populations Near Nuclear Weapons Test Sites Worldwide. vol 82.

Skipperud, L., 2004. Plutonium in the arctic marine environment—a short review. ScientificWorldJournal 4, 460–481.

Skwarzec, B., Struminska, D.I., Borylo, A., 2001. Bioaccumulation and distribution of plutonium in fish from Gdansk Bay. J. Environ. Radioact. 55, 167–178.

Smith, B.S., Child, D.P., Fierro, D., Harrison, J.J., Heijnis, H., Hotchkis, M.A.C., et al., 2016. Measurement of fallout radionuclides, ^{239,240}Pu and ^{137}Cs, in soil and creek sediment: Sydney Basin, Australia. J. Environ. Radioact. 151 (Part 3), 579–586.

Takata, H., Tagami, K., Aono, T., Uchida, S., 2014. Distribution coefficients (Kd) of strontium and significance of oxides and organic matter in controlling its partitioning in coastal regions of Japan. Sci. Total Environ. 490, 979–986.

Tims, S.G., Fifield, L.K., Hancock, G.J., Lal, R.R., Hoo, W.T., 2013. Plutonium isotope measurements from across continental Australia. Nucl. Inst. Methods Phys. Res. B 294, 636–641.
Tims, S.G., Froehlich, M.B., Fifield, L.K., Wallner, A., De Cesare, M., 2016. ^{236}U and $^{239,240}Pu$ ratios from soils around an Australian nuclear weapons test site. J. Environ. Radioact. 151, 563–567.
Tsukada, H., Takeda, A., Takahashi, T., Hasegawa, H., Hisamatsu, S., Inaba, J., 2005. Uptake and distribution of ^{90}Sr and stable Sr in rice plants. J. Environ. Radioact. 81, 221–231.
UNSCEAR, 2000. United Nations Scientific Committee on the Effects of Atomic Radiation, UNSCEAR 2000 Report to the General Assembly, with Scientific Annexes. Annex C, Vienna.
Whiting, S.D., Murray, W., Macrae, I., Thorn, R., Chongkin, M., Koch, A.U., 2008. Non-migratory breeding by isolated green sea turtles (Chelonia mydas) in the Indian Ocean: biological and conservation implications. Naturwissenschaften 95, 355–360.
Whiting, A.U., Thomson, A., Chaloupka, M., Limpus, C.J., 2009. Seasonality, abundance and breeding biology of one of the largest populations of nesting flatback turtles, Natator depressus: Cape Domett, Western Australia. Aust. J. Zool. 56, 297–303.
Wilcken, K.M., Hotchkis, M., Levchenko, V., Fink, D., Hauser, T., Kitchen, R., 2015. From carbon to actinides: a new universal 1MV accelerator mass spectrometer at ANSTO. Nucl. Instrum. Methods Phys. Res., Sect. B 361, 133–138.
Zheng, J., Tagami, K., Uchida, S., 2013. Release of plutonium isotopes into the environment from the Fukushima Daiichi nuclear power plant accident: what is known and what needs to be known. Environ. Sci. Technol. 47, 9584–9595.